In-situ FTIR spectroscopic study of the effect of CO_2 sorption on H-bonding in PEG-PVP mixtures

Labuschagne Ph., CSIR (South Africa) and Kazarian S.-G., Imperial College, London (United Kingdom)

Abstract

A study of the H-bonding between poly(ethylene glycol) (PEG) and polyvinylpyrrolidone (PVP) in the presence of supercritical carbon dioxide at various temperatures, pressures, different M_w of PEG and PVP and different PEG/PVP ratios is presented. *In-situ* attenuated total reflection Fourier transform infrared (ATR-FTIR) spectroscopy was used to investigate H-bonding by examining changes in the relative intensities and positions of peak maxima of the 2nd derivative ʋ(C=O) bands associated with 'free' and H-bound C=O groups. In general, relative intensities of bands associated with H-bound C=O groups decreased upon CO_2 sorption and was accompanied by an increase in intensity of bands associated with 'free' C=O groups. At the same time, these bands were shifted to higher wavenumbers. These shifts were attributed to the shielding effect of CO_2 molecules on H-bonding interactions between PEG and PVP. The magnitude of the effects of CO_2 shielding generally increased with decreasing polymer M_w and increasing CO_2 content. However, upon CO_2 venting the extent of the H-bonding between PEG and PVP reappeared. The extent of H-bonding recovery was greatest for blends with low M_w PEG (M_w: 4 x 10^2) and PVP (M_w: 9 x 10^3) and PEG content ≥ 0.54 wt% under mild conditions of pressure (80 bar) and temperature (35°C). For the same low M_w blends, increasing pressure to 150 bar, or temperature to 50°C, showed poor H-bond recovery upon CO_2 venting. Overall, it was shown that supercritical CO_2-induced shielding of H-bonding interactions in polymer blends is reversible upon CO_2 venting, and the magnitude of both was influenced by processing conditions and blend composition.

Keywords: supercritical fluids, ATR, FT-IR spectroscopy, H-bond, polymer blends

1. Introduction

Supercritical CO_2 has shown increased application as processing medium for polymers. Supercritical CO_2 is able to swell and plasticise polymers dramatically, allowing processes such as foaming[1], encapsulation[2], impregnation[3;4] and particle formation[5]. The high diffusivity of supercritical CO_2 combined with the ability to plasticise polymers allows it to act as a vehicle for the migration of various guest components into a polymer matrix[6-9]. In addition, the diffusivity and solvent power (which affects polymer plasticisation and swelling) is easily tuned with changes in pressure and temperature as evidenced by density-dependant polarity values[10]. This tunability allows for optimisation of process conditions.

A number of studies have indicated that increased CO_2 density leads to a decrease in inter-specie interaction or even phase separation of specifically interacting polymers. For instance, various authors have shown that the equilibrium constant for dimerization between molecules decreases with increased CO_2 pressure[11-13]. This decrease is most significant at densities above the critical density of the solvent. The decrease in dimerization is attributed to local density enhancement of CO_2 molecules around the reactants – generally referred to as solvent clustering.

Phase separation of specifically interacting polymers has also been shown to be due to CO_2 sorption. Walker et al (*14*) studied the effect of increased pressure on the phase behaviour of specifically interacting blends of amorphous poly(methyl methacrylate) (PMMA) and semi-crystalline poly(vinylidene fluoride) (PVDF). These polymers are believed to show strong specific interactions between their electric

moments and hydrogen-bond interactions between the electron-rich carbonyl oxygen of PMMA and the electron-poor hydrogen of PVDF. Blends were first compression moulded and then exposed to CO_2 at various pressures. Small-angle X-ray Scattering (SAXS) and Transmission Electron Microscopy (TEM) were used to investigate phase behaviour. At CO_2 pressures of up to 359 bar, no significant changes were noticed. However, at CO_2 pressures of 655 bar and higher, significant increases in scattering intensity were noticed, signifying the formation of ordered structures. In TEM images, the PVDF-rich dispersions showed increased definition and higher electron densities. This behaviour was more pronounced in blends with higher PVDF concentrations. Indications were that some PVDF fractions have aggregated to form lamellae. Two possible reasons were given for this behaviour: 1) at higher pressures, the CO_2 acts as a screen for intermolecular PVDF-PMMA interactions; 2) at higher pressures, the T_g of the blend (T_{gBLEND}) ($\approx 88°C$) was reduced to below the operating temperature of 35°C. This allows sufficient chain mobility for PVDF molecules to crystallise, thereby expelling PMMA molecules.

The phase behaviour of blends of weakly interacting poly(deuterated styrene) (d-PS) and poly(vinyl methyl ether) PVME was also investigated (*15*). These blends share weakly interactive charge-transfer interactions. The blends were prepared by first casting from a common solvent, dried, and then melt pressed into discs at 60°C. At ambient pressures and with no CO_2, the critical temperature (T_c) at which phase separation occurred for this blend was 155°C. After CO_2 sorption at a pressure of 240 bar, the T_c for this blend was reduced to 40°C. Using the Sanchez-Lacombe equation of state, it was estimated that at 240 bar, only about 3.3 wt% CO_2 was dissolved in the blend. Due to the very low CO_2 concentrations and weak CO_2 selectivity for any of the functional groups, it was concluded that the phase separation was not enthalpic-driven, but rather driven by entropic effects. This suggestion was based on evidence that a disparity existed in the degree of CO_2

sorption between d-PS and PMVE. Since compressibility of the blend increased rapidly with CO_2 sorption, the differential dilation of the two components lead to significant differences in their degrees of compressibility. These differences were believed to be the main cause of phase separation. The authors found similar behaviour between weakly interacting deuterated polybutadiene and polyisoprene blends (16). Phase segregation in this case was also attributed to disparities in compressibility of the two polymers after CO_2 sorption.

Fleming, Chan and Kazarian (17) studied supercritical CO_2 enhanced interdiffusion of poly(vinyl pyrrolidone) (PVP) and poly(ethylene glycol) (PEG). Films of PVP and PEG were cast alongside each other on a diamond ATR crystal. Interdiffusion was studied via FTIR-ATR images using a focal plane array detector and FTIR-ATR spectra themselves. Under atmospheric conditions, no interdiffusion was noticed as expected. At 40 and 80 bar, initial interdiffusion was noticed after 56 and 10 minutes respectively. The increased interdiffusion was explained as being due to increased chain mobility with higher CO_2 content. In this system, hydrogen bonding at the interface between PVP and PEG was also studied. In the absence of CO_2, the FTIR carbonyl band of PVP showed two conditions: unassociated carbonyl groups and associated (hydrogen-bonded) carbonyl groups. In this case, the carbonyl interacted with the terminal hydroxyl group in PEG. With increased CO_2 pressure, the hydrogen bonding interaction decreased as a result of a greater concentration of CO_2 molecules competing with the hydroxyl groups for carbonyl interaction. Based on this, they concluded that greater interdiffusion was due to both increased plasticisation and decreased intermolecular friction due to decreased hydrogen bond interactions.

However, the evolution of interaction behaviour of specifically interacting polymers under CO_2 pressure, and during CO_2 venting has not been studied in detail. The understanding of interaction behaviour during CO_2 processing; pressurisation,

maintaining of pressure, depressurisation, the effect of polymer molecular weight (M_w), polymer concentration etc. is important in optimizing process parameters.

In this study, the effect of dense CO_2 on hydrogen bonding interaction between the terminal hydroxyl groups of low molecular weight polyethylene glycol (PEG) and the carbonyl groups of polyvinylpyrrolidone (PVP) was monitored under various conditions with *in-situ* ATR-FTIR spectroscopy. The evolution of phase behaviour and hydrogen bond interaction in a CO_2 medium is pharmaceutically important for PEG and PVP blends. Such PEG-PVP networks have unique elastic and adhesive properties, making them suitable for use as transdermal delivery devices(*18*). This study would provide valuable information on the potential for preparing such networks in supercritical CO_2.

2. Experimental

2.1 Materials

PEG (400 and 1000 M_w) and PEG (600M_w) were purchased from Unilab and Fluka respectively. PVP Kollidon 17PF (±9 x 10^3 M_w), Kollidon 25PF (±3.1 x 10^4 M_w) and Kollidon F90 (±1.25 x 106 M_w) were purchased from BASF. Carbon dioxide (99.999% purity) was purchased from BOC Gases.

2.2 Methods

2.2.1 ATR-FTIR spectroscopy

An *in situ* ATR-FTIR spectroscopic approach which allows the simultaneous measurement of gas sorption and polymer swelling under high-pressure or supercritical CO_2 and which was developed at Imperial College London, UK was used in this study (*7;19*). A heated "Golden Gate" (diamond crystal with an incident

angle of 45°, ZnSe focusing lenses) was used. A specially designed "covering-cap" high-pressure cell, which was compatible with the single-reflection ATR accessories (Specac Ltd, UK), was used. All ATR-FTIR spectra were recorded with the use of a Bruker Equinox 55 FTIR spectrometer with a mercury-cadmium-telluride (MCT) detector. The resolution was 2 cm^{-1}.

2.2.2 Sample preparation

PEG and PVP raw materials were dried for 12 hours at 70°C in a vacuum oven (Model VO65, Vismara) prior to preparation of formulations. Formulations were prepared in order to study the effect of PEG terminal hydroxyl concentration, PEG and PVP molecular weights on H-bond interaction. To study the effect of PEG hydroxyl concentration, the PEG (PEG-400) and PVP (Kollidon 17PF) molecular weights were kept constant, while PEG400 concentration was varied: 0.36 wt%, 0.54 wt% and 0.72 wt%. To study the effect of PEG molecular weight, the PEG hydroxyl concentration and the PVP (Kollidon 17PF) molecular weights were kept constant, while PEG molecular weight was varied: 0.36 wt% PEG-400; 0.47 wt% PEG-600 and 0.6 wt% PEG-1000. To study the effect of PVP molecular weight, the PEG molecular weight (PEG-400) and PEG:PVP ratio was kept constant, while PVP molecular weight was varied: ~9 x 10^3 M_w(PVP-17PF), ~3.1 x 10^4 M_w (PVP-25PF) and ~1.25 x 10^6 M_w(PVP-F90).

Formulations were prepared by intimate mixing until visually homogenous (samples containing PEG-1000 were heated to above the PEG-1000 melting point prior to physical mixing). The samples were then sealed and allowed to condition for at least another 24 hours at ambient temperature before analysis.

2.2.3 Experimental procedure

The experimental approach was similar to the one described by Flichy et al. (*19*) and Fleming et al. (*7*). A spatula was used to transfer a small amount of prepared mixture onto the top surface of the ATR diamond inverted prism crystal. Sample sizes were kept similar to ensure good comparison between each experiment. The high-pressure cell was then carefully placed over the sample and sealed. For each prepared mixture, the first spectrum was obtained without CO_2. For spectra measured with CO_2, the absorbance of the CO_2 absorption peak at 2335 cm^{-1} was allowed to stabilise before the spectrum was collected.

3. Results and Discussion

A typical spectrum in the carbonyl absorption region of a PEG-PVP blend is shown in Figure 1A. This band is relatively broad, suggesting that it consists of a combination of overlapping bands. Resolving this band, by processing its second derivative, produces two bands (Fig 1B). Analysing the specific wavenumbers and relative intensities of these 2nd derivative bands allows for the detection of small variations in interaction behaviour between the different blend formulations and processing conditions. Second derivative spectra of the ν(C=O) absorption bands are thus used from here onwards to highlight subtle spectral differences.
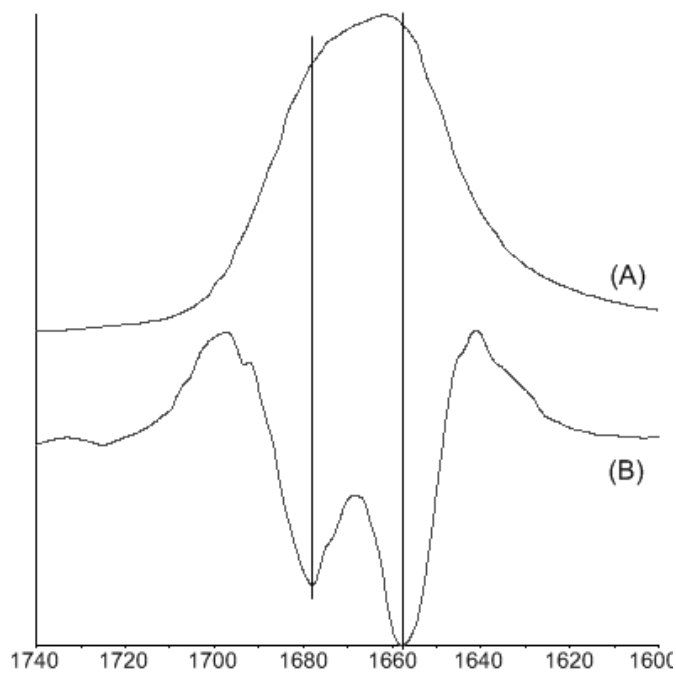
Figure 1: Absorption spectrum in the ν(C=O) region of a PVP blend with PEG (A), and its second derivative (B)

3.1 Effect of PEG concentration

Firstly, the effect of varying the PEG-400 concentration on H-bonding behaviour was studied. Since interaction between PEG and PVP molecules occurs via H-bond formation between the terminal hydroxyl group of PEG and the carbonyl group of PVP, spectral shifts involving the PVP ν(C=O) band were studied by ATR-FTIR spectroscopy. The range of hydroxyl stretching bands (3700 – 3200 cm^{-1}) was not considered because of the relatively weak absorbance in this region (due to the shallow penetration of IR light in the ATR at these wavenumbers) and because of the overlap of the spectral bands of PEG with the bands of water present in these samples.
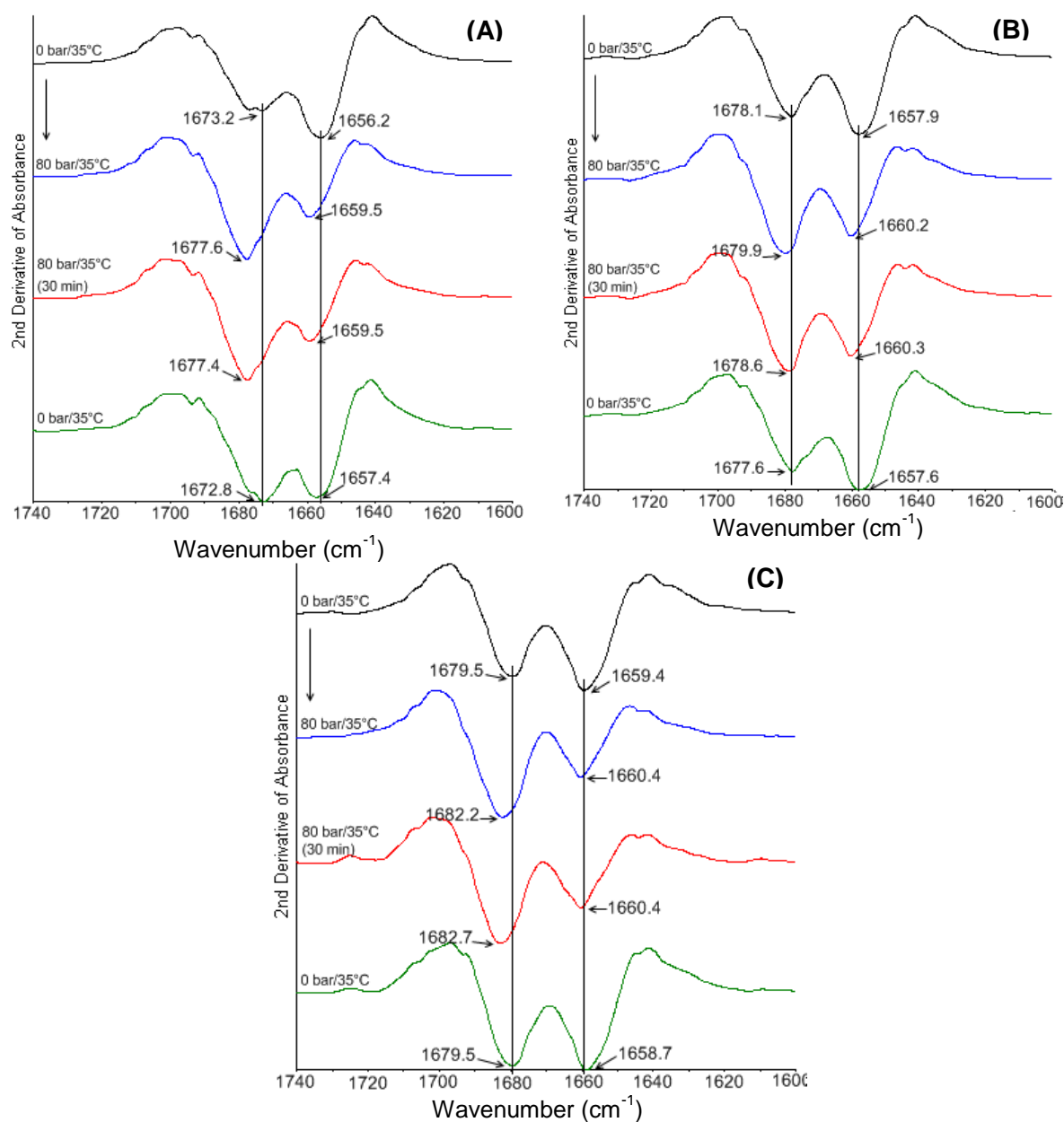
Figure 2: Second derivative profiles of the ATR-FTIR spectra representing the ʋ(C=O) bands for blends of PVP-17PF with PEG-400 loading at: (A) 0.36 wt%; (B) 0.54 wt%; (C) 0.72 wt%. (Vertical lines mark the peak maximum of corresponding bands before CO_2 sorption)

The second derivatives of the ʋ(C=O) absorption band consist of two prominent bands, the first band (ca 1678 cm^{-1}) representing non-H bonded or 'free' carbonyl groups and the second band (ca 1656 cm^{-1}) representing carbonyl groups that are H-

bonded to PEG-400 (*7*). The blend with 0.36 wt% PEG-400 shows an additional band at 1673 cm^{-1} prior to CO_2 sorption, which could be attributed to PVP-PVP dipole interaction resulting from closer packing at low PEG-400 concentration(*20*) (Fig. 2). Consequently, as the PEG-400 concentration increases, this band disappears. Prior to CO_2 sorption, H-bonding strength appears strongest for blends with 0.36 wt% PEG-400 and decreases with increasing PEG-400 concentration, as illustrated by the ʋ(C=O) band of H-bound carbonyl groups being shifted to higher wavenumbers with increasing PEG-400 concentration. Increasing PEG-400 concentration also leads to the ʋ(C=O) band of 'free' carbonyl groups shifting to higher wavenumbers. It is possible that at higher PEG-400 concentration, a greater number of PEG-PEG H-bonds occur at the expense of PEG interacting with PVP. Also, increased PEG concentration leads to a greater concentration of oxyethylene units, which repel PVP carbonyl groups.

For all PEG-400 concentrations, initial CO_2 pressurisation up to 80 bar shows an increase in the relative intensity of ʋ(C=O) band of 'free' carbonyl groups and a complimentary decrease in the relative intensity of the ʋ(C=O) band of H-bound carbonyl groups. This can be attributed to competition between PEG terminal hydroxyl groups and CO_2 molecules for interaction with the PVP carbonyl groups (*7*). In addition, the strength of the remaining H-bond interactions is weakened as illustrated by the peak maximum of the ʋ(C=O) band of H-bound carbonyl groups, thereby shifting to higher wavenumbers. It is possible that clustering of weakly interacting CO_2 molecules around the oxyethylene units of PEG chains results in some steric shielding. As a result, polar PEG terminal hydroxyl groups are spatially shielded by CO_2 molecules. Interestingly, upon CO_2 venting, the relative intensity of the ʋ(C=O) band of the H-bound carbonyl groups increases again. This indicates that the shielding effect of supercritical CO_2 is reversible upon venting. In fact, the peak maximum of the ʋ(C=O) band of H-bound carbonyl groups for 0.54 wt% and 0.72

wt% PEG-400 shifts to slightly lower wavenumbers than seen prior to CO_2 sorption, while for the 0.36 wt% PEG-400, this band returns to a slightly higher wavenumber. This implies that, under low supercritical CO_2 pressure, the blend remains largely homogenous with PEG chains dispersed between the PVP chains, but separated by CO_2 molecules. During CO_2 venting, the inter-chain distances and the supercritical CO_2 shielding effects decrease, and imparts sufficient mobility for PEG-400 hydroxyl groups to interact with PVP carbonyl groups.

In order to emphasize the effect of different PEG-400 concentrations on interaction behaviour, variations in the relative intensities of the second derivative bands representing H-bound (I_h) and 'free' (I_f) carbonyl groups upon CO_2 pressurisation and venting, were analysed. The ratios of these relative intensities (I_h/I_f) are plotted in Figure 3. The values were normalised to an initial value of 1 to improve comparison:
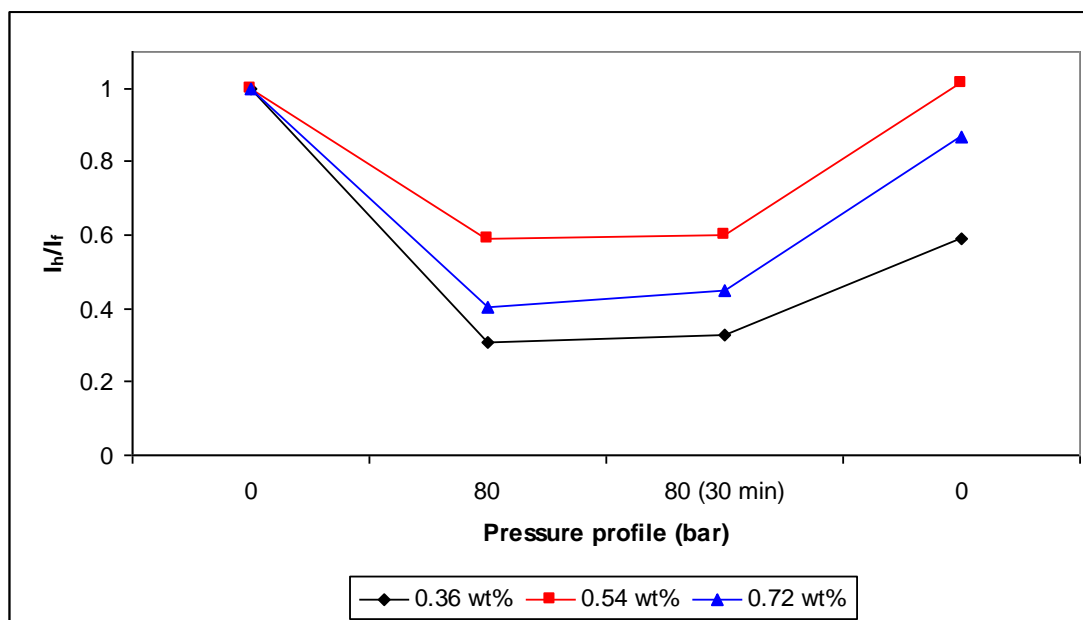

Figure 3: Ratios of relative intensities of ν(C=O) bands representing H-bound (I_h) and 'free' (I_f) carbonyl groups derived from second derivative spectra as a function of PEG-400 concentration in PVP-17PF. (Normalised to initial value of 1 for comparison).

The blend with 0.36 wt% PEG-400 shows the biggest decrease in the I_h/I_f ratio upon CO_2 sorption and also displayed the poorest recovery, while the blend with 0.54 wt% PEG-400 shows the highest recovery when compared to original I_h/I_f ratios after CO_2 venting. Due to increased CO_2 solubility in PEG, increasing PEG-400 concentration leads to increased dissolved CO_2. Chain mobility is thus increased, which would increase the potential for favourable PEG-400 and PVP chain rearrangement, allowing a higher degree of PEG-PVP interaction to be maintained. However, increased CO_2 concentration is also associated with increased supercritical CO_2-induced shielding of PEG-PVP interactions, as illustrated by the poor recovery in I_h/I_f ratios of the blend with 0.72 wt% PEG-400 when compared to the blend with 0.54 wt% PEG-400. Thus, it appears an optimum PEG-400 concentration exists for maximising PEG-PVP H-bond interaction upon CO_2 venting. Figure 3 also shows a slight increase in the I_h/I_f ratio after 30 minutes at 80 bar which is the result of increased chain mobility that allows some degree of H-bond interactions to occur.

3.2 Effect of PEG Molecular Weight

Samples were also prepared to determine the effect of molecular weight of PEG on H-bonding, while keeping concentration of the PEG terminal hydroxyl groups constant.
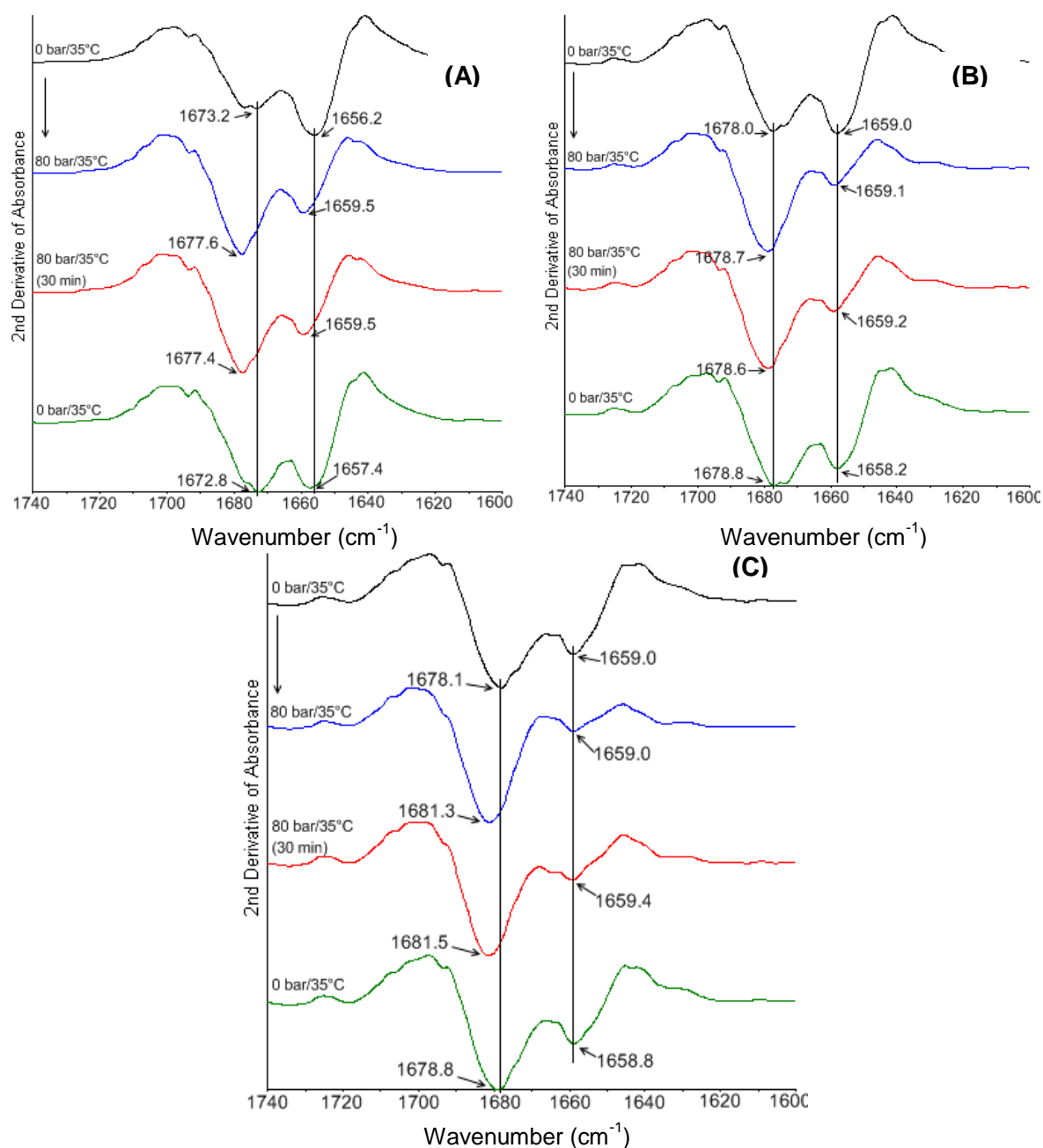
Figure 4: Second derivative profiles of the ATR-FTIR spectra representing the ʋ(C=O) bands for blends of PVP-17PF with: (A) PEG-400 (0.36 wt%); (B) PEG-600 (0.47 wt%); (C) PEG-1000 (0.6 wt%). (Vertical lines mark the peak maximum of the corresponding bands before CO_2 sorption).

Figure 4(A) shows that prior to CO_2 sorption, stronger H-bond strength in blends containing PEG-400 and also higher relative intensity of the ʋ(C=O) band of H-

bound carbonyl groups were experienced when compared to blends with PEG-600 and PEG-1000. Blends containing PEG-1000 show the highest relative intensity of the ν(C=O) band of 'free' carbonyl groups. These differences can be attributed to entropy effects. By increasing PEG molecular weight, the combinatorial entropy of the blend is reduced, and strong H-bond interactions are less favoured. In addition, increasing PEG molecular weight also increases the concentration of oxyethylene units, which not only competes with PVP carbonyl groups for H-bond interaction with PEG terminal hydroxyl groups, but also repels PVP carbonyl groups.

With CO_2 sorption and desorption, into and out, of the PEG-PVP blends, the same general trend is repeated as before. CO_2 sorption leads to a reduced PEG-PVP interaction as illustrated by a decrease in the intensity of the ν(C=O) band of H-bound carbonyl groups, and a corresponding increase in intensity of the ν(C=O) band of 'free' carbonyl groups. Upon CO_2 desorption, this process is reversed.

However, important differences in the I_h/I_f ratios are visible. With initial CO_2 sorption up to 80 bar pressure, increased PEG molecular weight is accompanied by decreased I_h/I_f ratios (Fig. 5). This can be attributed to various factors. Apart from a weaker initial H-bond strength between PEG and PVP, increased PEG molecular weight also increases the concentration of oxyethylene units, which in turn leads to increased CO_2 sorption. This increases the shielding of H-bond interactions between PEG and PVP.
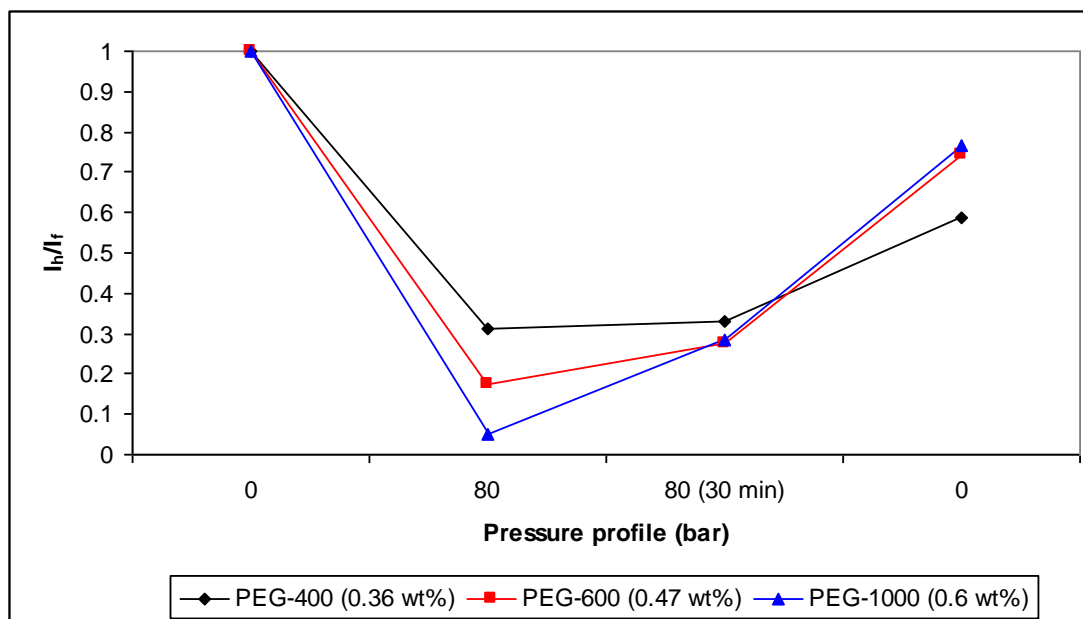
Figure 5: Ratios of relative intensities of ν(C=O) bands representing H-bound (I_h) and 'free' (I_f) carbonyl groups derived from second derivative spectra as a function of PEG M_w in blends with PVP-17PF (Normalised to initial value of 1 for comparison).

Interestingly though, the blends containing PEG-1000 show the highest increase in the I_h/I_f ratio after 30 minutes at 80 bar. This is possibly the result of increased CO_2 concentration that allows a greater degree of polymer chain mobility and rearrangement. During such rearrangement, PEG-1000 and PVP chains approach each other and given a favourable orientation, leads to H-bond interactions. The increased chain mobility of the blends with high molecular weight PEG also allows greater recovery in I_h/I_f ratios after CO_2 venting.

3.3 Effect of molecular weight of PVP
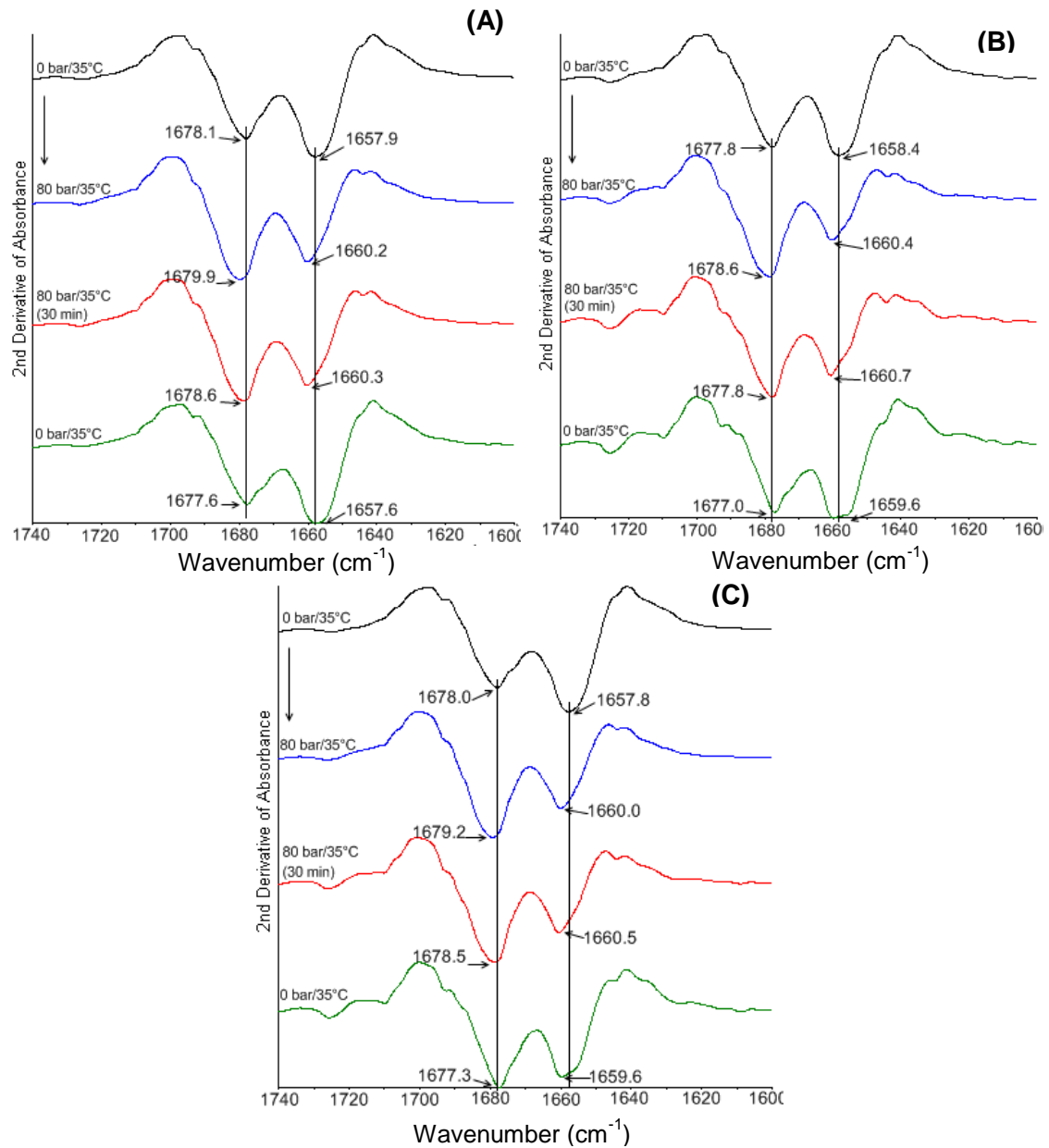
Figure 6: Second derivative profiles of the ATR-FTIR spectra representing the υ(C=O) bands for blends of PEG-400 (0.54 wt%) with: (A) PVP-17PF; (B) PVP-25PF; (C) PVP-F90. (Vertical lines mark the peak maximum of the corresponding bands before CO_2 sorption).

As with the previous blends, CO_2 pressurisation leads to an increase in relative intensity of the ν(C=O) band of 'free' carbonyl groups and a corresponding decrease in relative intensity of the ν(C=O) band of H-bound carbonyl groups. All blends, irrespective of PVP molecular weight, also show equal shifts in their peak maxima of the ν(C=O) bands for both 'free' and H-bound carbonyl groups upon CO_2 sorption. Following CO_2 venting however, the blend containing the low molecular weight PVP (PVP-17PF) shows the fullest recovery to its original H-bond strength with PEG. Again, this can be attributed to improved chain mobility of the low molecular weight PVP that allows for a greater degree of rearrangement for optimal PEG-PVP interaction. The impact of varying PVP molecular weight is emphasized by comparing the I_h/I_f ratios of the respective blends (Fig. 7)
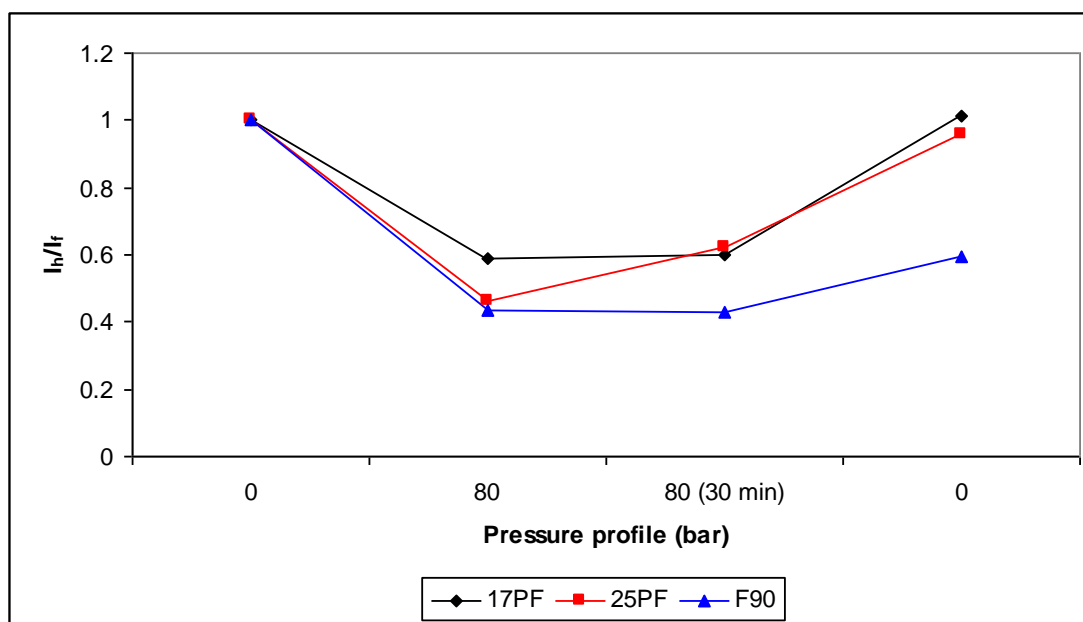

Figure 7: Ratios of relative intensities of ν(C=O) bands representing H-bound (I_h) and 'free' (I_f) carbonyl groups derived from second derivative spectra as a function of PVP M_w in blends with PEG-400 (0.54 wt%). (Normalised to initial value of 1 for comparison).

Figure 7 shows that for blends containing the higher molecular weight PVP-F90 (M_w: 1.25 x 10^6), the I_h/I_f *recovery* is the poorest (I_h/I_f = 0.59), while blends containing PVP-17PF and PVP-25PF show I_h/I_f ratios 1.02 and 0.96 respectively. If it is assumed that the amount of absorbed CO_2 in these blends are similar (since PEG concentrations were kept constant), it is evident that by decreasing polymer molecular weight, supercritical CO_2-assisted rearrangement and subsequent collision of PEG and PVP chains are enhanced, resulting in greater H-bond interaction after CO_2 venting.

It is also interesting to note that the blend with intermediate PVP molecular weight (M_w: 3.1 x 10^4) shows the greatest "ageing" effect when maintaining CO_2 pressure at 80 bar. It is expected that the rate of supercritical CO_2-assisted rearrangement will decrease with increasing PVP molecular weight, as higher molecular weight PVP molecules impose kinetic restrictions on the mobility of PEG molecules. At low PVP molecular weight (M_w: 9 x 10^3), these restrictions are almost insignificant, and rearrangement (assisted by CO_2 molecules) occurs at such a rate that it is almost complete when 80 bar CO_2 pressure is reached. Increasing PVP molecular weight slows down the rate of rearrangement, resulting in delayed rearrangement after initial pressurisation to 80 bar. With very high PVP molecular weight (M_w: 1.25 x 10^6), rearrangement either does not occur, or occurs too slowly for any difference in I_h/I_f ratios to be noted after 30 minutes at 80 bar CO_2 pressure.

3.4 Effect of Changing Temperature and Pressure

The effect of increasing temperature to 50 °C and CO_2 pressure to 150 bar on the interaction between PEG and PVP was studied. Figure 8 shows the effect of temperature and pressure on the spectral shifts of the ν(C=O) bands for blends containing 0.54 wt% PEG-400 in PVP-F90 and 0.47 wt% PEG-600 in PVP-F90:
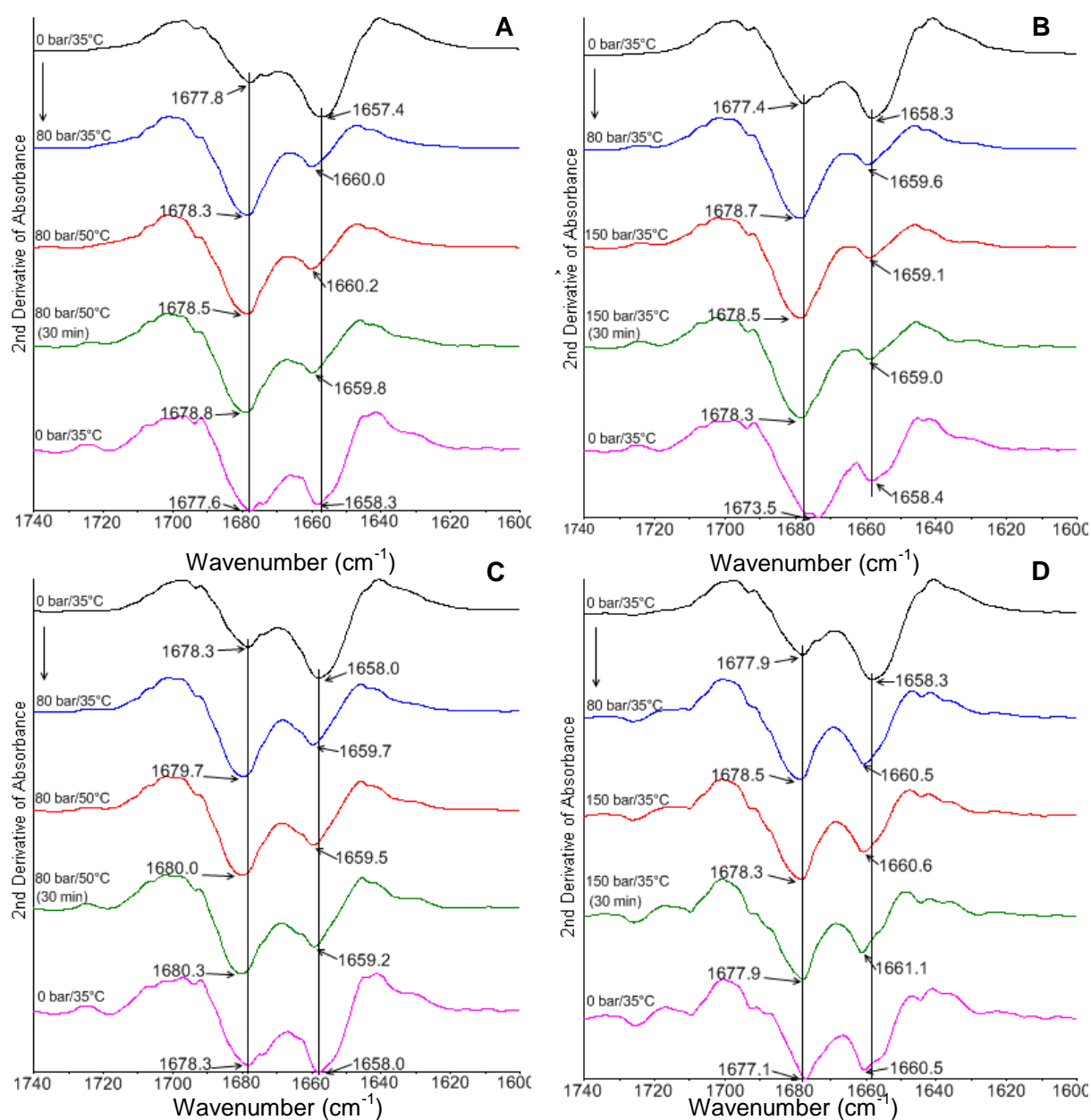
Figure 8: Second derivative profiles of ATR-FTIR spectra representing the ν(C=O) bands for PEG-600/PVP-17PF blends: (A) temperature effect, (B) pressure effect and PEG-400/PVP-F90 blends: (C) temperature effect, (D) pressure effect. (Vertical lines represent maximum of band intensity before CO_2 sorption)

For all blends, similar shifts in the peak maximum of the ν(C=O) bands of both 'free' and H-bound carbonyl groups are shown, irrespective of temperature or pressure

variations. The only notable difference is seen in the ν(C=O) bands of 'free' carbonyl groups after CO_2 venting. Prior to CO_2 sorption, all these bands have a shoulder at ca. 1673 cm^{-1} which has previously been attributed to weak PVP-PVP dipole interactions, indicating that close packing of PVP chains occurs in some areas. These band shoulders are slightly more pronounced in blends containing PEG-600, which is probably an indication of slightly less favourable interaction with PVP due to the increased PEG molecular weight. Following CO_2 venting at the more severe conditions of temperature and pressure, these band shoulders become more pronounced. Furthermore, it is noticeable from Figure 8 that the intensities of the ν(C=O) band of H-bound carbonyl groups are significantly reduced after CO_2 venting, suggesting reduced PEG-PVP interaction. The evidence of both increased PVP-PVP dipole interaction and reduced PEG-PVP H-bond interaction could suggest that some degree of phase separation had occurred. The only blend in which evidence of PVP-rich phases is less pronounced upon CO_2 venting, is in the PEG-400/PVP-F90 blend that was exposed to 150 bar CO_2 pressure. It is possible that PEG molecules are trapped in the high molecular weight PVP matrix, thereby reducing their ability to self-diffuse. This in turn, prevents close packing of PVP chains. Further effects of changing CO_2 pressure and temperature are emphasized by plotting I_h/I_f ratios (Fig. 9):
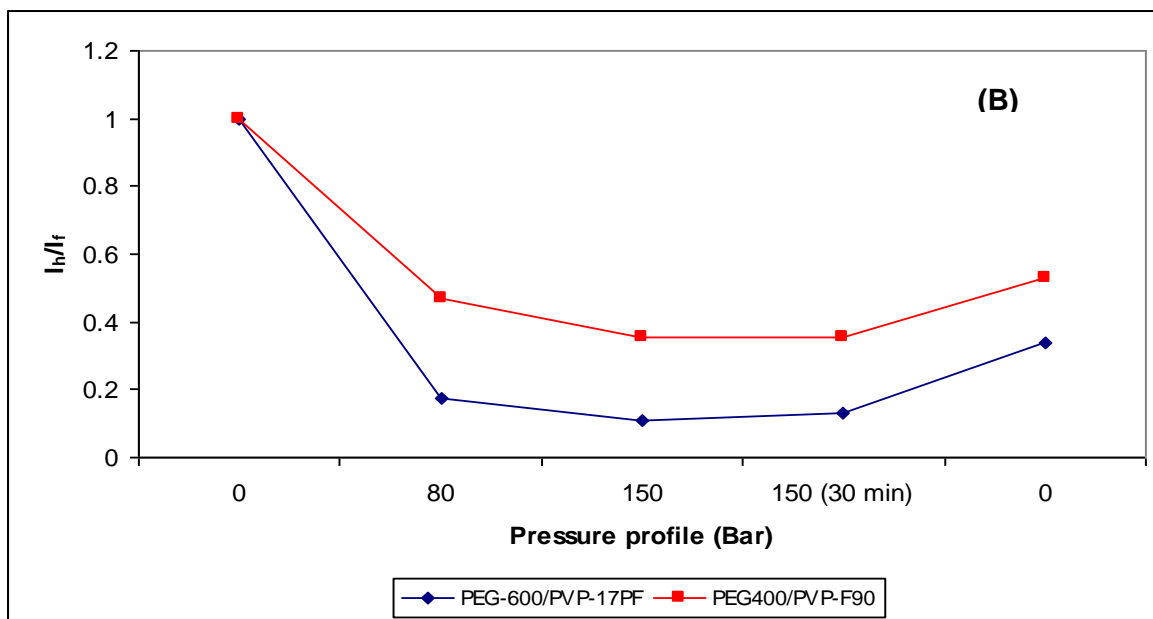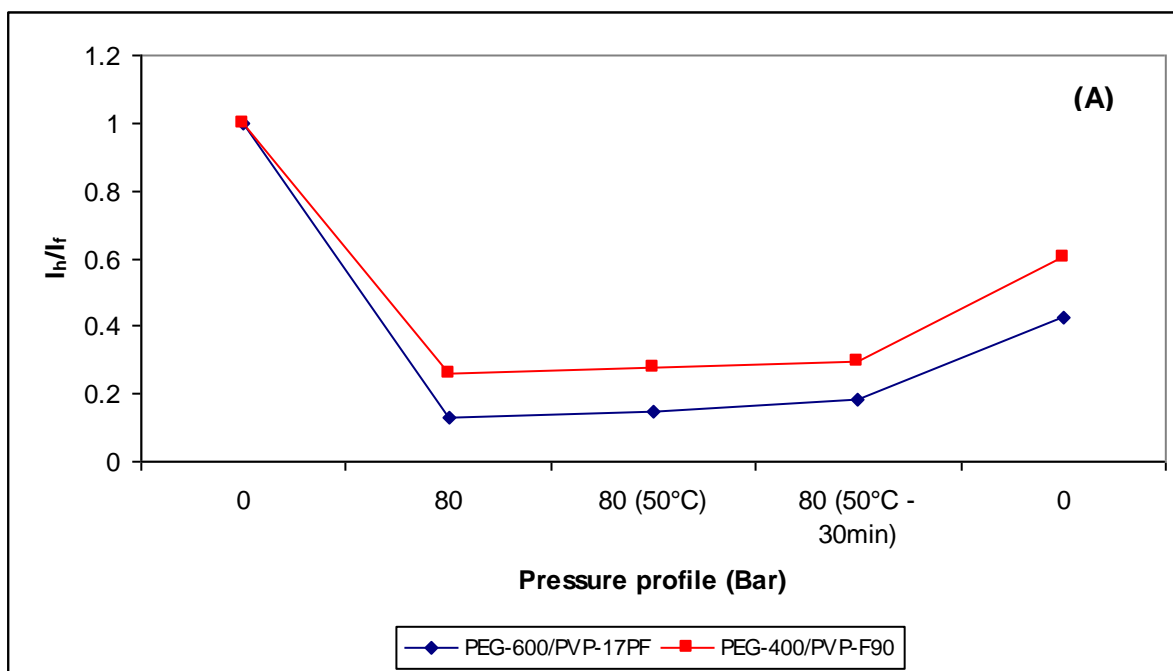
Figure 9: Effect of temperature (A) and CO_2 pressure (B) on the ratios of relative intensities of ν(C=O) bands representing H-bound (I_h) and 'free' (I_f) carbonyl groups of two PEG-PVP blends derived from second derivative spectra. (Normalised to initial value of 1 for comparison).

Figure 9 shows that increasing temperature actually results in a slight increase in the I_h/I_f ratio. On the contrary, increasing CO_2 pressure shows a decrease in I_h/I_f ratios. These effects can easily be explained thus: By increasing temperature, the concentration of CO_2 dissolved in the blends is decreased, reducing the shielding of PEG-PVP interactions. By increasing pressure, the concentration of CO_2 dissolved in the polymers is increased, thus increasing the CO_2 shielding effect of PEG-PVP interactions.

Another observation is that blends of PEG-600/PVP-17PF show overall reduced I_h/I_f ratios when compared to PEG-400/PVP-F90 blends. This can be attributed to the low PVP molecular weight in the PEG-600/PVP-17PF blends, since increased CO_2 solubility in polymers with lower molecular weight should result in enhanced masking effect of interactions(21). Interesting though, is that the discrepancy in I_h/I_f values remain even after CO_2 venting. The reason for this could be two-fold. Firstly, H-bond activity for PEG-PVP blends is inversely proportional to PEG molecular weight due to entropy effects. Secondly, the low PVP molecular weight poses less restriction to mobility of polymer chains. The combination of these effects is likely to result in some degree of phase separation, as is supported by evidence of increased PVP-PVP dipole interaction.

4. Conclusions

In-situ ATR-FTIR spectroscopic analysis has shown that in all the PEG-PVP blends studied, irrespective of processing variables, CO_2 sorption leads to a reduction in intermolecular H-bonding interaction between PVP and PEG. This is demonstrated by the second derivative spectra of the $\nu(C=O)$ absorption band showing a decrease in intensity of the band representing H-bound carbonyl groups and a corresponding increase in intensity of the band representing 'free' carbonyl groups. The decreased

interaction is attributed to the increased amount of dissolved CO_2 molecules that effectively screen the PEG and PVP molecules from one another. The strength of such H-bond shielding is affected by polymer molecular weight, concentration of functional groups interacting with CO_2 molecules, processing pressure and temperature. In general it is shown that, the higher the concentration of CO_2 dissolved in the polymer and the lower the molecular weight of the polymer blend, the greater the shielding effect.

Interestingly, during CO_2 venting, H-bonding interactions between PEG and PVP reappear, indicating the reversibility of supercritical CO_2 induced masking effects. It is believed that during CO_2 venting, masking effects are reduced, yet sufficient mobility is provided for PEG and PVP molecules to rearrange and form H-bonds with one another.

The extent of PEG-PVP interaction recovery upon CO_2 venting was found to be dependant on a number of factors. Generally, blends of PEG/PVP with a PEG content $\geq$ 0.54 wt% and a low M_w PVP (9×10^3) under mild pressure (80 bar) and temperature (35°C) conditions show very good interaction recovery. However, by further increasing the CO_2 pressure (150 bar) or processing temperature (50°C), H-bond interaction recovery for low molecular weight blends is severely restricted with evidence of possible phase separation. Seemingly, an optimum CO_2 concentration and polymer chain mobility exists for yielding a PEG-PVP blend with a greater number of H-bond interactions.

Acknowledgements

References

1. Goel, S. K. and Beckman, E. J. (1994) Generation of microcellular polymeric foams using supercritical carbon dioxide. II: cell growth and skin formation, *Polymer Engineering and Science 34*, 1148-1156.

2. Kim, J. H., Paxton, T. E., and Tomasko, D. L. (1996) Microencapsulation of naproxen using rapid expansion of supercritical solutions, *Biotechnology Progress 12*, 650-661.

3. Kikic, I. and Vecchione, F. (2003) Supercritical impregnation of polymers, *Current Opinion in Solid State and Materials Science 7*, 399-405.

4. Cooper, A. I., Kazarian, S. G., and Poliakoff, M. (1993) Supercritical fluid impregnation of polyethylene films, a new approach to studying equilibria in matrices; the hydrogen bonding of fluoroalcohols to $(\eta^5$-$C_5Me_5)Ir(CO)_2$ and the effect on C⋯H activation, *Chemical Physics Letters 206,* 175-180.

5. Yeo, S. D. and Kiran, E. (2005) Formation of polymer particles with supercritical fluids: A review, *Journal of Supercritical Fluids 34*, 287-308.

6. Ngo, T. T., Liotta, C. L., Eckert, C. A., and Kazarian, S. G. (2003) Supercritical fluid impregnation of different azo-dyes into polymer: In situ UV/Vis spectroscopic study, *Journal of Supercritical Fluids 27*, 215-221.

7. Fleming, O. S., Chan, K. L. A., and Kazarian, S. G. (2006) High-pressure CO_2-enhanced polymer interdiffusion and dissolution studied with in situ ATR-FTIR spectroscopic imaging, *Polymer 47*, 4649-4658.

8. Kazarian, S. G. (1997) Applications of FTIR spectroscopy to supercritical fluid drying, extraction and impregnation, *Applied Spectroscopy Reviews 32*, 301-348.

9. Kazarian, S. G., Brantley, N. H., and Eckert, C. A. (1999) Dyeing to be clean: Use supercritical carbon dioxide, *CHEMTECH 29*, 36-41.

10. Sigman, M. E., Lindley, S. M., and Leffler, J. E. (1985) Supercritical carbon dioxide: Behavior of n* and β solvatochromic indicators in media of different densities, *Journal of the American Chemical Society 107*, 1471-1472.

11. Bell, P. W., Thote, A. J., Park, Y., Gupta, R. B., and Roberts, C. B. (2003) Strong Lewis Acid-Lewis Base Interactions between Supercritical Carbon Dioxide and Carboxylic Acids: Effects on Self-association, *Industrial and Engineering Chemistry Research 42*, 6280-6289.

12. Xu, Q., Han, B., and Yan, H. (1999) Equilibrium Constant and Enthalpy for the Hydrogen Bonding of Acetic Acid with Tetrahydrofuran in Supercritical CO_2, *Journal of Physical Chemistry A 103*, 5240-5245.

13. Mu, T., Han, B., Zhang, J., Li, Z., Liu, Z., Du, J., and Liu, D. (2004) Hydrogen bonding of acetic acid in CO_2 + n-pentane mixed fluids in the critical region, *Journal of Supercritical Fluids 30*, 17-24.

14. Walker, T. A., Melnichenko, Y. B., Wignall, G. D., Lin, J. S., and Spontak, R. J. (2003) Phase behavior of poly(methyl methacrylate)/poly(vinylidene fluoride) blends in the presence of high-pressure carbon dioxide, *Macromolecular Chemistry and Physics 204*, 2064-2077.

15. Watkins, J. J., Brown, G. D., RamachandraRao, V. S., Pollard, M. A., and Russell, T. P. (1999) Phase separation in polymer blends and diblock copolymers induced by compressible solvents, *Macromolecules 32*, 7737-7740.

16. RamachandraRao, V. S., Vogt, B. D., Gupta, R. R., and Watkins, J. J. (2003) Effect of carbon dioxide sorption on the phase behavior of weakly interacting polymer mixtures: Solvent-induced segregation in deuterated polybutadiene/polyisoprene blends, *Journal of Polymer Science Part B-Polymer Physics 41*, 3114-3126.

17. Fleming, O. S., Chan, K. L. A., and Kazarian, S. G. (2006) High-pressure CO2-enhanced polymer interdiffusion and dissolution studied with in situ ATR-FTIR spectroscopic imaging, *Polymer 47*, 4649-4658.

18. Feldstein, M. M., Tohmakhchi, V. N., Malkhazov, L. B., Vasiliev, A. E., and Plat+¬, N. A. (1996) Hydrophilic polymeric matrices for enhanced transdermal drug delivery, *International Journal of Pharmaceutics 131*, 229-242.

19. Flichy, N. M. B., Kazarian, S. G., Lawrence, C. J., and Briscoe, B. J. (2002) An ATR-IR study of poly (dimethylsiloxane) under high-pressure carbon dioxide: Simultaneous measurement of sorption and swelling, *Journal of Physical Chemistry B 106*, 754-759.

20. Chiu, C. Y., Yen, Y. J., Kuo, S. W., Chen, H. W., and Chang, F. C. (2007) Complicated phase behavior and ionic conductivities of PVP-co-PMMA-based polymer electrolytes, *Polymer 48*, 1329-1342.

21. Elvassore, N., Vezzù, K., and Bertucco, A. (2005) Measurement and modeling of CO_2 absorption in poly(lactic-co-glycolic acid), *The Journal of Supercritical Fluids 33*, 1-5.